Taylor & Francis
Taylor & Francis Group

REPORT

🔓 OPEN ACCESS | Check for updates |

Characterization of anti-SARS-CoV-2 monoclonal antibodies focusing on antigen binding, neutralization, and FcγR activation via formation of immune complex

Minoru Tada (iD), Michihiko Aoyama, and Akiko Ishii-Watabe

Division of Biological Chemistry and Biologicals, National Institute of Health Sciences, Kawasaki, Japan

ABSTRACT

Severe acute respiratory syndrome coronavirus 2 (SARS-CoV–2) causes coronavirus disease 2019 (COVID–19). Antibodies induced by SARS-CoV–2 infection or vaccination play pivotal roles in the body's defense against the virus; many monoclonal antibodies (mAbs) against SARS-CoV–2 have been cloned, and some neutralizing mAbs have been used as therapeutic drugs. In this study, we prepared an antibody panel consisting of 31 clones of anti-SARS-CoV–2 mAbs and analyzed and compared their biological activities. The mAbs used in this study were classified into different binding classes based on their binding epitopes and showed binding to the SARS-CoV–2 spike protein in different binding kinetics. A multiplex assay using the spike proteins of Alpha, Beta, Gamma, Delta, and Omicron variants clearly showed the different effects of variant mutations on the binding and neutralization activities of different binding classes of mAbs. In addition, we evaluated Fcγ receptor (FcγR) activation by immune complexes consisting of anti-SARS-CoV–2 mAb and SARS-CoV–2 pseudo-typed virus, and revealed differences in the FcγR activation properties among the binding classes of anti-SARS-CoV–2 mAbs. It has been reported that FcγR-mediated immune-cell activation by immune complexes is involved in the promotion of immunopathology of COVID–19; therefore, differences in the FcγR-activation properties of anti-SARS-CoV–2 mAbs are among the most important characteristics when considering the clinical impacts of anti-SARS-CoV–2 mAbs.

Introduction

Antibodies play a pivotal role in humoral immunity for fighting viral infections, and monoclonal antibodies (mAbs) are promising therapeutics for the prevention and treatment of infectious diseases.[1] The coronavirus disease 2019 (COVID–19) pandemic has accelerated efforts to develop neutralizing mAbs that target severe acute respiratory syndrome coronavirus 2 (SARS-CoV–2). Recent advances in antibody discovery technologies such as single-cell analysis and next-generation sequencing (NGS) have enabled researchers to isolate the mAbs quite rapidly and have allowed the cloning of more mAbs targeting SARS-CoV–2 than ever before.[2] As of December 2022, 12004 antibodies had been registered in the Coronavirus Antibody Database (CoV-AbDab; opig.stats.ox.ac.uk/webapps/covabdab), and some of these anti-SARS-CoV–2 therapeutic mAb products received Emergency Use Authorization from the US Food and Drug Administration.[3,4]

Most of the anti-SARS-CoV–2 neutralizing mAbs bind to the receptor-binding domain (RBD) of the SARS-CoV–2 spike protein, thereby blocking viral binding to angiotensin-converting enzyme 2 (ACE2) on host cells. The SARS-CoV–2 spike protein forms a trimer, and RBDs exist in two conformational states, described as "up" (open) and "down" (closed).[5,6] In the up conformation, the receptor binding motif (RBM) on the RBD is exposed for ACE2 binding. Several classifications for RBD-binding mAbs based on binding

epitopes have been suggested.[4,7,8] In general, anti-RBD mAbs are classified into four groups: Class 1 mAbs recognize the RBM on the up conformation RBD, mimicking the binding to ACE2. Class 2 mAbs can bind the RBM in both up- and down-state RBDs. Class 3 mAbs bind outside the ACE2-binding site of RBD (RBD core cluster I), while class 4 mAbs bind to the opposite surface of the RBD (RBD core cluster II). The binding structures of representative mAbs (class 1, REGN10933; class 2, P2B–2F6; class 3, REGN10987; class 4, CR3022) to the SARS-CoV–2 spike RBD are shown in Figure 1a.

Since the beginning of the COVID–19 pandemic, SARS-CoV–2 variants with genetic mutations that affect viral characteristics have appeared, with new variants continually emerging.[11,12] Several mutations in the spike protein of SARS-CoV–2 variants have been found to reduce the neutralization activity of mAbs, resulting in viral evasion of mAb-mediated protection.[7,11,13,14] The mutations located at RBD in variants of concern (VOCs) are shown in Figure 1b. Effects of the mutations in VOCs on the neutralization activity of anti-SARS-CoV–2 mAbs have been well studied. For example, E484K (a glutamate (E)-to-lysine (K) substitution at position 484 in the RBM) of the Beta variant (B.1.351) is identified as an escape mutation reducing the binding affinity of anti-SARS-CoV–2 antibodies in convalescent sera.[15,16] E484A (a glutamate (E) -to-
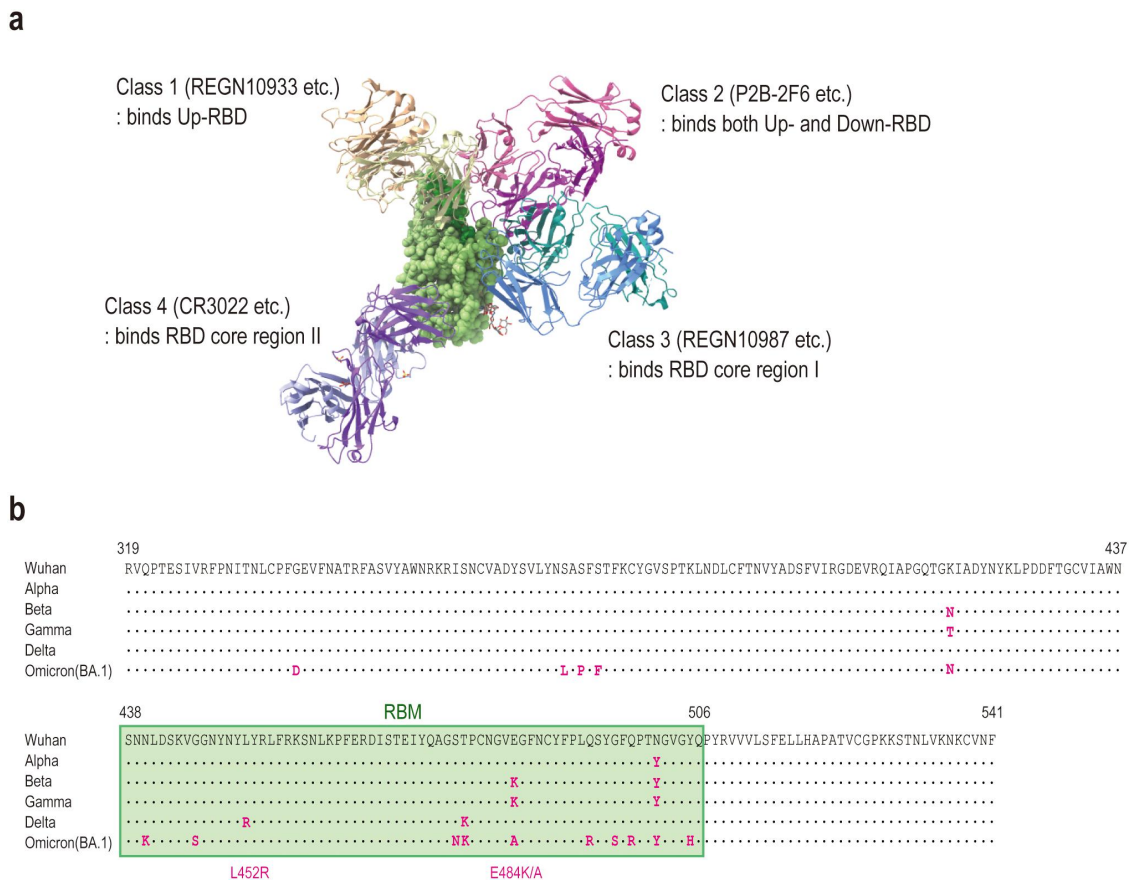
Figure 1. (a) Structure of anti-SARS-CoV−2 Fabs bound to a spike RBD. The image was generated using UCSF ChimeraX[9,10] by superimposing the structures of REGN10933/REGN10987 (PDB ID: 6×DG), P2B − 2F6 (PDB ID: 7BWJ) and CR3022 (PDB ID: 6W41). The RBD is shown by the green surface, and Fabs in different binding classes are shown as cartoons of different colors. (b) the mutations located at spike protein RBD in Alpha, Beta, Gamma, Delta, and Omicron BA.1 variants are shown. The sequence corresponding to RBM is highlighted in green.

alanine (A) substitution at the same position) is found in Omicron (B.1.1.529) and its subvariants, and is known to contribute to resistance to neutralization by anti-SARS-CoV−2 mAbs in combination with other mutations.[17,18] There are numerous studies[11–14,17,19,20] examining the impacts of variant mutations on the activity of anti-SARS-CoV−2 mAbs, and these have contributed to the ongoing effort to understand and defend against new variants using mAb-based therapeutics.

In this study, we prepared an antibody panel consisting of 31 clones of recombinant anti-SARS-CoV−2 mAbs to compare their biological activities against SARS-CoV−2. This panel includes previously reported clones of anti-SARS-CoV−2 mAbs, as well as therapeutic mAbs with various characteristics in binding affinity, binding classes with different epitopes, and neutralization activity. An analysis of the binding and neutralization activities against various SARS-CoV−2 variants revealed the impacts of these mutations on the biological activities of mAbs in different binding classes. We also analyzed Fcγ receptor (FcγR) activation by immune complexes consisting of anti-SARS-CoV−2 mAbs and a SARS-CoV−2 pseudo-typed virus, and revealed differences in FcγR-mediated immune-cell activation by anti-SAR-CoV−2 mAbs bound to SARS-CoV−2.

Results

Preparation of recombinant anti-SARS-CoV−2 mAbs

To prepare our panel of anti-SARS-CoV−2 mAbs, 31 clones of previously described mAbs were selected, and their sequences were obtained from the Protein Data Bank (PDB) or the World Health Organization's designated International Nonproprietary Names (INN) (Table 1). Most of these mAbs had been cloned before the emergence of SARS-CoV−2 variants and are known to bind to the spike protein of the original Wuhan strain. This panel includes the clones of therapeutic mAbs: mAb01 (bamlanivimab), mAb02 (casirivimab), mAb03 (imdevimab), mAb09 (etesevimab), mAb28 (cilgavimab), mAb29 (regdanivimab), mAb30 (sotrovimab) and mAb31 (tixagevimab). To exclude the influences of differences other than antigen-binding properties, cDNA sequences of antibody-variable regions were subcloned into human IgG1-expressing plasmids, and recombinant mAbs with human IgG1 subclass were prepared using CHO cells. The binding affinity to the SARS-CoV−2 (Wuhan) spike protein was evaluated by surface plasmon resonance (SPR) analysis. The recombinant anti-SARS-CoV−2 mAbs bound to the spike protein with various binding kinetics, as shown in Figure 2.

Table 1. mAbs used in this study.

|	Variable Region	Binding Class	PDB	Reference
mAb01	bamlanivimab	2	-	INN
mAb02	casirivimab	1	6×DG	Hansen et al. Science 369, 1010–1014 (2020)[21]
mAb03	imdevimab	3		
mAb04	CR3022	4	6W41	Yuan et al. Science 368, 630–633 (2020)[22]
mAb05	P2B–2F6	2	7BWJ	Ju et al. Nature 584, 115–119 (2020)[23]
mAb06	S309	3	6WPS	Pinto et al. Nature 583, 290–295 (2020)[24]
mAb07	BD–23	2	7BYR	Cao et al. Cell 182, 73–84 (2020)[25]
mAb08	B38	1	7BZ5	Wu et al. Science 368, 1274–1278 (2020)[26]
mAb09	etesevimab	1	7C01	Shi et al. Nature 584, 120–124 (2020)[27]
mAb10	52	2	7K9Z	Rujas et al. Nat Commun 12, 3661–3661 (2021)[28]
mAb11	298	1		
mAb12	C102	1	7K8M	Barnes et al. Nature 588, 682–687 (2020)[29]
mAb13	C135	3	7K8R	
mAb14	C002	2	7K8S	
mAb15	C119	2	7K8W	
mAb16	C121	2	7K8X	
mAb17	C144	2	7K90	
mAb18	CV07–250	1	6×KQ	Kreye et al. Cell 183, 1058–1069 (2020)[30]
mAb19	CV07–270	2	6×KP	
mAb20	S2H13	2	7JV4	Piccoli et al. Cell 183, 1024–1042 (2020)[31]
mAb21	S2A4	4	7JVC	
mAb22	S304	4	7JW0	
mAb23	COVA1–16	4	7JMW	
mAb24	S2E12	1	7K3Q	Tortorici et al. Science 370, 950–957 (2020)[32]
mAb25	S2M11	2	7K43	
mAb26	4A8	NTD	7C2L	Chi et al. Science 369, 650–655 (2020)[33]
mAb27	H014	4	7CAK	Lv et al. Science 369, 1505–1509 (2020)[34]
mAb28	cilgavimab	3	-	INN
mAb29	regdanvimab	1	-	INN
mAb30	sotrovimab	3	-	INN
mAb31	tixagevimab	1	-	INN
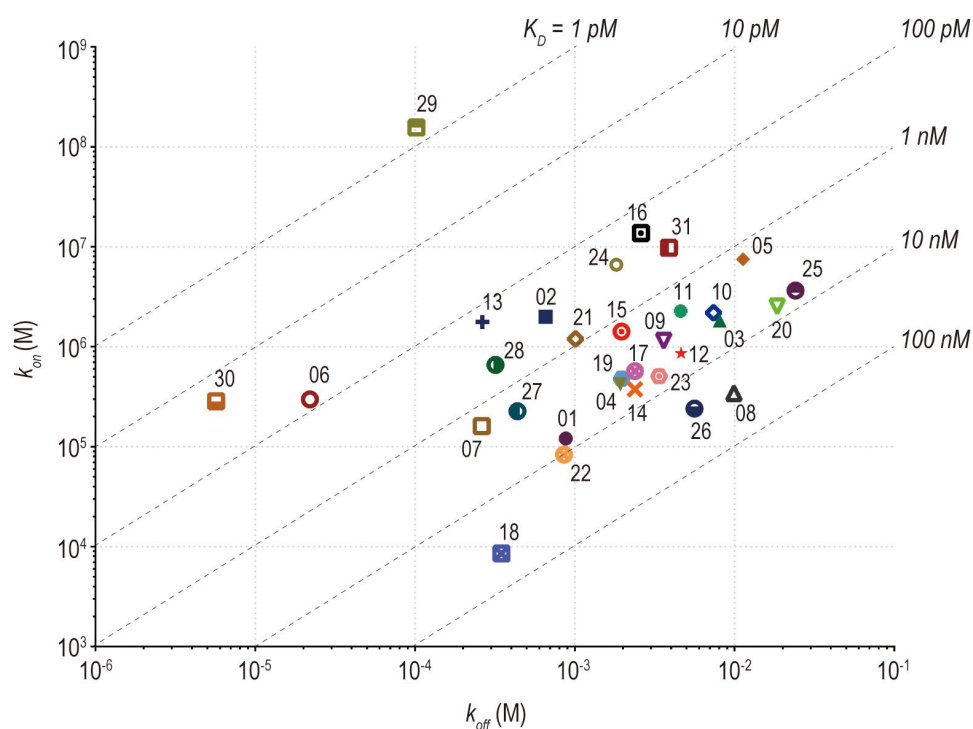
Figure 2. An on-off rate map indicating the binding kinetics parameters of anti-SARS-CoV −2 mAbs against Wuhan spike protein analyzed by SPR analysis. The association rate constant (k_{on}) is plotted against the dissociation rate constant (k_{off}). The diagonal lines indicate the equilibrium dissociation constant (K_D).

Binding and neutralization activity to SARS-CoV−2 variants

For a comprehensive evaluation of the biological activities of anti-SARS-CoV−2 mAbs, antigen-binding and neutralization activities were analyzed by an electrochemiluminescence (ECL) multiplex assay using the spike proteins of SARS-CoV−2 variants: Wuhan, Alpha (B.1.1.7), Beta (B.1.351), Gamma (P.1), Delta (B.1.617.2), and Omicron (B.1.1.529). Binding activities were assessed by measuring the degree of mAbs binding to immobilized spike proteins, and neutralization activities were assessed by measuring the inhibition of human ACE2 binding to the immobilized spike proteins. Rituximab, an anti-CD20 mAb, was used as the negative control. Dose – response curves of binding and neutralization are shown in Supplemental Figures 1 and 2, respectively. Area under the curve (AUC) values were calculated and are shown in Figure 3. All 31 clones of anti-SARS-CoV−2 mAbs used in this study showed binding to the Wuhan spike protein, whereas their binding activities against the variants' spike proteins varied widely among the clones. Although the neutralization activity
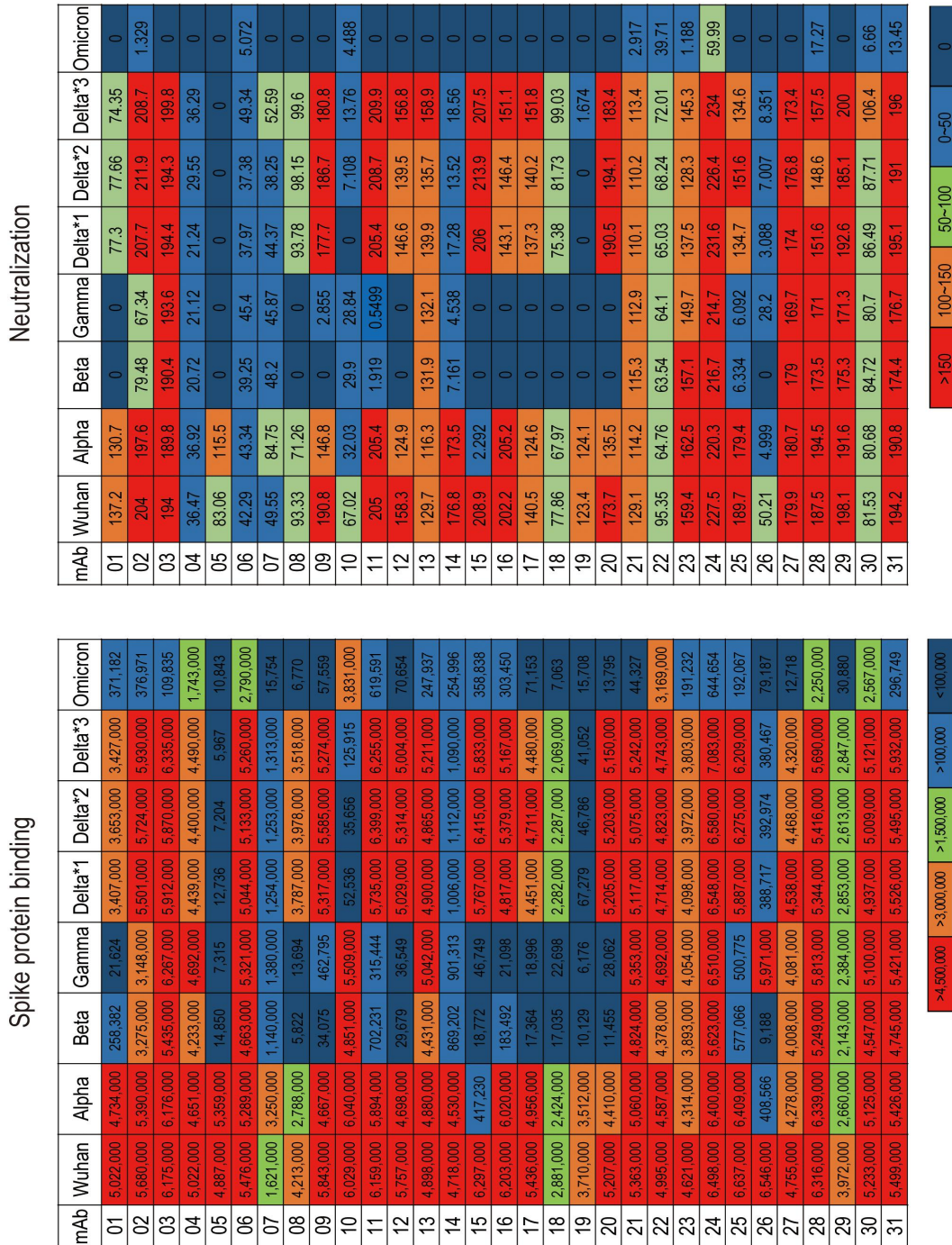
Neutralization

mAb	Wuhan	Alpha	Beta	Gamma	Delta*1	Delta*2	Delta*3	Omicron
01	137.2	130.7	0	0	77.3	77.66	74.35	0
02	204	197.6	79.48	67.34	207.7	211.9	208.7	1.329
03	194	189.8	190.4	193.6	194.4	194.3	199.8	0
04	36.47	36.92	20.72	21.12	21.24	29.55	36.29	0
05	83.06	115.5	0	0	0	0	0	0
06	42.29	43.34	39.25	45.4	37.97	37.38	49.34	5.072
07	49.55	84.75	48.2	45.87	44.37	38.25	52.59	0
08	93.33	71.26	0	0	93.78	98.15	99.6	0
09	190.8	146.8	29.9	2.855	177.7	186.7	180.8	0
10	67.02	32.03	1.919	28.84	0	7.108	13.76	4.488
11	205	205.4	0	0.5499	205.4	208.7	209.9	0
12	158.3	124.9	0	0	146.6	139.5	156.8	0
13	129.7	116.3	131.9	132.1	139.9	135.7	158.9	0
14	176.8	173.5	7.161	4.538	17.28	13.52	18.56	0
15	208.9	2.292	0	0	206	213.9	207.5	0
16	202.2	205.2	0	0	143.1	146.4	151.1	0
17	140.5	124.6	0	0	137.3	140.2	151.8	0
18	77.86	67.97	0	0	75.38	81.73	99.03	0
19	123.4	124.1	0	0	0	0	1.674	0
20	173.7	135.5	0	0	190.5	194.1	183.4	0
21	129.1	114.2	115.3	112.9	110.1	110.2	113.4	2.917
22	95.35	64.76	63.54	64.1	65.03	68.24	72.01	39.71
23	159.4	162.5	157.1	149.7	137.5	128.3	145.3	1.188
24	227.5	220.3	216.7	214.7	231.6	226.4	234	59.99
25	189.7	179.4	6.334	6.092	134.7	151.6	134.6	0
26	50.21	4.999	0	28.2	3.088	7.007	8.351	0
27	179.9	180.7	179	169.7	174	176.8	173.4	0
28	187.5	194.5	173.5	171	151.6	148.6	157.5	17.27
29	198.1	191.6	175.3	171.3	192.6	185.1	200	0
30	81.53	80.68	84.72	80.7	86.49	87.71	106.4	6.66
31	194.2	190.8	174.4	176.7	195.1	191	196	13.45

Color scale: 0 | 0–50 | 50~100 | 100~150 | >150

Spike protein binding

mAb	Wuhan	Alpha	Beta	Gamma	Delta*1	Delta*2	Delta*3	Omicron
01	5,022,000	4,734,000	258,382	21,624	3,407,000	3,653,000	3,427,000	371,182
02	5,680,000	5,390,000	3,275,000	3,148,000	5,501,000	5,724,000	5,930,000	376,971
03	6,175,000	6,176,000	5,435,000	6,267,000	5,912,000	5,870,000	6,335,000	109,835
04	5,022,000	4,651,000	4,233,000	4,692,000	4,439,000	4,400,000	4,490,000	1,743,000
05	4,887,000	5,359,000	14,850	7,315	12,736	7,204	5,967	10,843
06	5,476,000	5,289,000	4,663,000	5,321,000	5,044,000	5,133,000	5,260,000	2,790,000
07	1,621,000	3,250,000	1,140,000	1,380,000	1,254,000	1,253,000	1,313,000	15,754
08	4,213,000	2,788,000	5,822	13,694	3,787,000	3,978,000	3,518,000	6,770
09	5,843,000	4,667,000	34,075	462,795	5,317,000	5,585,000	5,274,000	57,559
10	6,029,000	6,040,000	4,851,000	5,509,000	52,536	35,656	125,915	3,831,000
11	6,159,000	5,894,000	702,231	315,444	5,735,000	6,399,000	6,265,000	619,591
12	5,757,000	4,698,000	29,679	36,549	5,029,000	5,314,000	5,004,000	70,654
13	4,898,000	4,880,000	4,431,000	5,042,000	4,900,000	4,865,000	5,211,000	247,937
14	4,718,000	4,530,000	869,202	901,313	1,006,000	1,112,000	1,090,000	254,996
15	6,297,000	417,230	18,772	46,749	5,767,000	6,415,000	5,833,000	358,838
16	6,203,000	6,020,000	183,492	21,098	4,817,000	5,379,000	5,167,000	303,450
17	5,436,000	4,956,000	17,364	18,996	4,451,000	4,711,000	4,480,000	71,153
18	2,881,000	2,424,000	17,035	22,698	2,282,000	2,287,000	2,069,000	7,063
19	3,710,000	3,512,000	10,129	6,176	67,279	46,786	41,052	15,708
20	5,207,000	4,410,000	11,455	28,062	5,205,000	5,203,000	5,150,000	13,795
21	5,363,000	5,060,000	4,824,000	5,353,000	5,117,000	5,075,000	5,242,000	44,327
22	4,995,000	4,587,000	4,378,000	4,692,000	4,714,000	4,823,000	4,743,000	3,169,000
23	4,621,000	4,314,000	3,893,000	4,054,000	4,098,000	3,972,000	3,803,000	191,232
24	6,498,000	6,400,000	5,623,000	6,510,000	6,548,000	6,580,000	7,083,000	644,654
25	6,637,000	6,409,000	577,066	500,775	5,887,000	6,275,000	6,209,000	192,067
26	6,546,000	408,566	9,188	5,971,000	388,717	392,974	380,467	79,187
27	4,755,000	4,278,000	4,008,000	4,081,000	4,538,000	4,468,000	4,320,000	12,718
28	6,316,000	6,339,000	5,249,000	5,813,000	5,344,000	5,416,000	5,690,000	2,250,000
29	3,972,000	2,660,000	2,143,000	2,384,000	2,853,000	2,613,000	2,847,000	30,880
30	5,233,000	5,125,000	4,547,000	5,100,000	4,937,000	5,009,000	5,121,000	2,567,000
31	5,499,000	5,426,000	4,745,000	5,421,000	5,526,000	5,495,000	5,932,000	296,749

Color scale: <100,000 | >100,000 | >1,500,000 | >3,000,000 | >4,500,000

Figure 3. Binding and neutralization activities against spike proteins of SARS-CoV −2 variants. AUCs calculated from the dose–response curves of spike protein binding assay (Supplement Figure 1) and neutralization assay (Supplement Figure 2) are shown. Spike proteins from the following lineages were used in the assay: Wuhan, Alpha (B.1.1.7), Beta (B.1.351), Gamma (P.1), Delta *1 (B.1.617.2; AY.4), Delta *2 (B.1.617.2; AY.4.2), Delta *3 (B.1.617.2; AY.3; AY.5; AY.6; AY.7; AY.14) and Omicron (B.1.1.529; BA.1).

		Wuhan	Alpha	Beta	Gamma	Delta*1	Delta*2	Delta*3	Omicron
Class 1	mAb02	100.0	94.9	57.7	55.4	96.8	100.8	104.4	6.6
	mAb08	100.0	66.2	0.1	0.3	89.9	94.4	83.5	0.2
	mAb09	100.0	79.9	0.6	7.9	91.0	95.6	90.3	1.0
	mAb11	100.0	95.7	11.4	5.1	93.1	103.9	101.6	10.1
	mAb12	100.0	81.6	0.5	0.6	87.4	92.3	86.9	1.2
	mAb18	100.0	84.1	0.6	0.8	79.2	79.4	71.8	0.2
	mAb24	100.0	98.5	86.5	100.2	100.8	101.3	109.0	9.9
	mAb29	100.0	67.0	54.0	60.0	71.8	65.8	71.7	0.8
	mAb31	100.0	98.7	86.3	98.6	100.5	99.9	107.9	5.4
Class 2	mAb01	100.0	94.3	5.1	0.4	67.8	72.7	68.2	7.4
	mAb05	100.0	109.7	0.3	0.1	0.3	0.1	0.1	0.2
	mAb07	100.0	200.5	70.3	85.1	77.4	77.3	81.0	1.0
	mAb10	100.0	100.2	80.5	91.4	0.9	0.6	2.1	63.5
	mAb14	100.0	96.0	18.4	19.1	21.3	23.6	23.1	5.4
	mAb15	100.0	6.6	0.3	0.7	91.6	101.9	92.6	5.7
	mAb16	100.0	97.0	3.0	0.3	77.7	86.7	83.3	4.9
	mAb17	100.0	91.2	0.3	0.3	81.9	86.7	82.4	1.3
	mAb19	100.0	94.7	0.3	0.2	1.8	1.3	1.1	0.4
	mAb20	100.0	84.7	0.2	0.5	100.0	99.9	98.9	0.3
	mAb25	100.0	96.6	8.7	7.5	88.7	94.5	93.6	2.9
Class 3	mAb03	100.0	100.0	88.0	101.5	95.7	95.1	102.6	1.8
	mAb06	100.0	96.6	85.2	97.2	92.1	93.7	96.1	50.9
	mAb13	100.0	99.6	90.5	102.9	100.0	99.3	106.4	5.1
	mAb28	100.0	100.4	83.1	92.0	84.6	85.8	90.1	35.6
	mAb30	100.0	97.9	86.9	97.5	94.3	95.7	97.9	49.1
Class 4	mAb04	100.0	92.6	84.3	93.4	88.4	87.6	89.4	34.7
	mAb21	100.0	94.4	89.9	99.8	95.4	94.6	97.7	0.8
	mAb22	100.0	91.8	87.6	93.9	94.4	96.6	95.0	63.4
	mAb23	100.0	93.4	84.2	87.7	88.7	86.0	82.3	4.1
	mAb27	100.0	90.0	84.3	85.8	95.4	94.0	90.9	0.3
NTD	mAb26	100.0	6.2	0.1	91.2	5.9	6.0	5.8	1.2

100 80 60 40 20 0
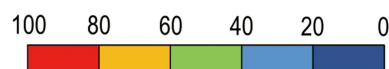
Figure 4. Comparison of the binding activities to spike proteins of SARS-CoV −2 variants among mAbs of different binding classes. The relative binding activities (%) were calculated by normalizing the AUCs of binding to variant spike proteins by those to the Wuhan spike protein. Relative binding (% against Wuhan) to Alpha (B.1.1.7), Beta (B.1.351), Gamma (P.1), Delta *1 (B.1.617.2; AY.4), Delta *2 (B.1.617.2; AY.4.2), Delta *3 (B.1.617.2; AY.3; AY.5; AY.6; AY.7; AY.14) and Omicron (B.1.1.529; BA.1) are shown for each binding class.

against Wuhan differed among the clones, the results suggested that decreased binding activities strongly contributed to the reduction of neutralization activities.

To clarify the different effects of the variant mutations, the relative binding activities to variant spike proteins of each mAb (as a percentage of those of Wuhan) were calculated. As shown in Figure 4, decreases in binding activity to the variant spike proteins were relatively dependent on the binding class of the mAbs. In class 1, remarkable diminishments

were observed in the binding to Beta, Gamma, and Omicron variants: 5 of the 9 clones showed less than 20% binding to the Beta and Gamma variants while all 9 clones showed less than 20% binding to the Omicron variant. In class 2, less than 20% binding was observed in 9 of the 11 clones to the Beta and Gamma variants, 3 of the 11 clones to Delta subvariants and 10 of the 11 clones to the Omicron variant. On the other hand, all clones in classes 3 and 4 showed more than 80% binding to Beta, Gamma, and Delta variants. Although 2 of the 5 clones in
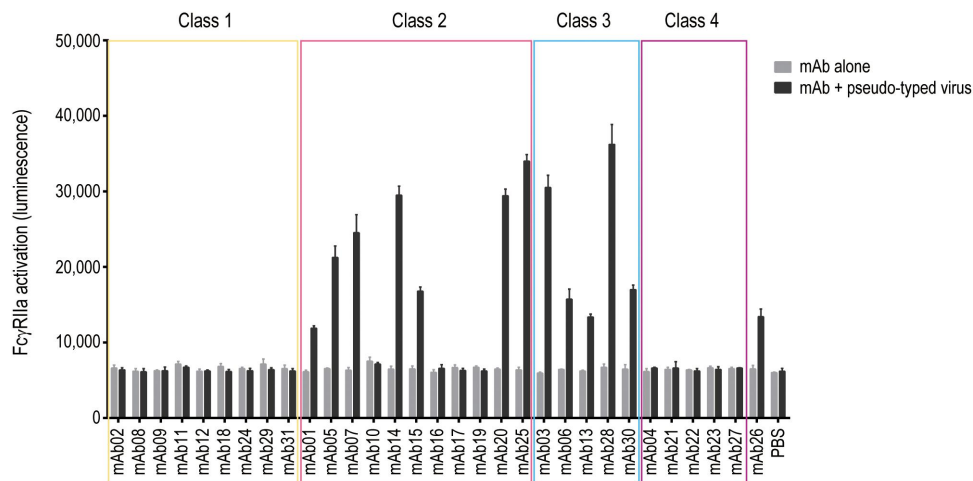
Figure 5. FcγRIIa activation by immune complexes consisting of anti-SARS-CoV−2 mAbs and SARS-CoV−2 pseudo-typed virus. FcγRIIa activation was measured using Jurkat/FcγRIIa/NFAT-Luc reporter cells. Data represent means + SEMs (*n* = 3).

class 3 and 3 of the 5 clones in class 4 showed less than 20% binding to the Omicron variant, mAbs in classes 3 and 4 were relatively resistant in their binding to SARS-CoV−2 variants compared to those in class 1 and 2. mAb26, which bound to the N-terminal domain (NTD) in the spike protein, showed less than 20% binding to all variants except for Gamma.

We next prepared SARS-CoV−2 (Wuhan) spike pseudo-typed virus and measured the neutralization activities of representative mAbs against the pseudo-typed virus. The mAbs used in this study showed different neutralization activities (Supplemental Figure 3a), and a positive correlation (R square = 0.867) was observed between the AUC calculated from the pseudo-typed virus neutralization assay and the ACE−2 binding-inhibition assay (Supplemental Figure 3b).

FcγRIIa activation by the immune complexes consisting of anti-SARS-CoV−2 mAbs and SARS-CoV−2 spike pseudo-typed virus

Immune complexes formed by antigen-bound antibodies can activate immune cells via FcγRs, inducing inflammatory responses or elimination of the antigen.[35,36] We have previously reported that reporter cell lines expressing human FcγRs (hFcγR) and a luciferase reporter driven by NFAT (NFAT-Luc) were useful for evaluating immune-cell activation via FcγRs.[37−39] Using a reporter cell line (Jurkat/hFcγRIIa/NFAT-Luc), we next assessed FcγRIIa activation by immune complexes consisting of anti-SARS-CoV−2 mAbs and SARS-CoV−2 (Wuhan) spike pseudo-typed virus (Figure 5). We first confirmed that neither the mAbs alone nor the pseudo-typed virus alone was able to activate hFcγRIIa. Interestingly, FcγRIIa-activation properties differed among the various binding classes of mAbs. Immune complexes formed by mAbs in classes 1 and 4 did not activate hFcγRIIa in our assay condition, whereas 7 of the 11 clones in class 2 and all 5 clones in class 3 showed activation of hFcγRIIa.

Discussion

During the global spread of COVID−19, the efficacy of antibodies induced by vaccinations or administered as therapeutic

drugs has been dramatically affected by the mutations in SARS-CoV−2 variants. There have been numerous studies of the influences of variant mutations, and several mutations have been identified as so-called "escape" mutations.[3,7,14] Especially, mutations in the RBD were shown to directly reduce the binding of anti-SARS-CoV−2 antibodies that target the RBD. In this study, we prepared a panel consisting of 31 clones of anti-SARS-CoV−2 mAbs, and evaluated their binding and neutralization activities to the major SARS-CoV−2 variants. Our results clearly indicated differences in the effects of variant mutations among the binding classes of mAbs. Distinct decreases in the binding to Beta and Gamma variants were observed in class 1 and 2 mAbs, but not in class 3 and 4 mAbs. Beta and Gamma variants contain an escape mutation, E484K in the RBM, which is the target of class 1 and 2 mAbs; this explains the reduction of binding activities of class 1 and 2 mAbs. The L452R (a leucine (L) -to-arginine (R) substitution at position 452) mutation present in the Delta variant is also located in the RBM and has been shown to reduce the binding activities of some RBM-targeting mAbs.[7,19,20] In our experiment, moderate (>20%) to strong (>80%) decreases in the binding to the Delta variant were observed in some mAbs in classes 1 and 2. The decreases were more evident in class 2 mAbs than class 1 mAbs, a result consistent with those of a previous report by Deshpande et al.[7] In the Omicron variant, further mutations are present in both the RBM and the core region of RBD. Significant decreases in binding were observed not only in class 1 and 2 mAbs but also in classes 3 and 4 mAbs, which target core regions of the RBD. The effects of variant mutations on the neutralization activities measured by the inhibition of ACE2-spike protein binding showed similar trends to those on the binding activities. As a note of caution, the results obtained from an assay using recombinant proteins do not necessarily reflect the neutralization activities against authentic viral infections. However, we have revealed the characteristics of each binding class in terms of biological activities against SARS-CoV−2 variants. It is true that the effects of variant mutations on the biological activities of anti-RBD mAbs are not fully explained only by their binding class, the binding epitopes (linear epitopes) are important for

considering the effects of variants' mutations. Nevertheless, our results, which were consistent with those of previous reports, should be helpful for understanding the impacts of variant mutations on the efficacy of anti-SARS-CoV−2 mAbs.

Fc-mediated effector functions are among the most important roles of antibodies in the immune system.[36] Antibodies bound to antigens form immune complexes and can activate immune cells via FcγRs, inducing the engulfment and elimination of antigens or the inflammatory responses. In this study, we revealed the differences in the FcγRIIa-activation properties of immune complexes consisting of anti-SARS-CoV−2 mAbs and SARS-CoV−2 pseudo-type virus, and the results indicated the possibility that the FcγR-activation properties differed depending on the binding class of mAbs. To examine these differences from a structural perspective, we generated binding models of antibody antigen-binding fragments (Fabs) bound to SARS-CoV−2 spike proteins. SARS-CoV−2 spike proteins form a trimeric structure, and spike trimers exist in open or closed conformations at the pre-fusion state. In the open conformation, the RBD of one or two spike monomer(s) is exposed (i.e., the "up" conformation) and available for binding to ACE−2.[5,6] Structural models of anti-SARS-CoV−2 mAb Fabs bound to the spike trimer in a two up conformation are shown in Figure 6. Class 1 mAbs can only bind to the RBD in the up conformation; thus, only two or fewer Fab molecules can bind to a spike trimer. In addition, the binding model of REGN10933 indicated the possibility that simultaneous binding of two Fab molecules might be blocked by steric hindrance. On the other hand, Class 2 mAbs bind both up- and down-state RBDs, and up to three Fab molecules could bind a spike trimer in either the open or closed conformation. Class 3 mAbs bind to the outer face of the RBD core region, and three Fab molecules could bind to a spike trimer as shown in the case of REGN10987. Class 4 mAbs bind to the inner face of the RBD and require large conformational changes of spike proteins for their binding;[40] hence, it seems unlikely that

multiple Fab molecules could bind a spike trimer simultaneously. These binding models suggested that more Fab molecules of mAbs in classes 2 and 3 than in classes 1 and 4 could simultaneously bind a SARS-CoV−2 spike trimer in either the open or closed form. Considering the bivalent binding of IgG, an antibody can bind a spike trimer at two binding sites or bridge two neighboring spike proteins. The multiple-binding ability of mAbs in classes 2 and 3 to a spike trimer may contribute to the clustering of spike trimers on the viral membrane, resulting in the multimerization of the antibody Fc region. Because the activation of FcγRs is triggered by multimeric Fc binding, it is possible that the immune complexes of mAbs in classes 2 and 3 could activate FcγRs more efficiently than those of mAbs in class 1 and 4.

Although FcγR-mediated immune-cell activation by antibodies is related to potent defense mechanisms against foreign pathogens, it has been reported that FcγR-driven inflammatory responses might be associated with the immunopathology of COVID−19. Ankerhold et al. have reported that excessive FcγR activation by circulating immune complexes is involved in the promotion of immunopathology in severe or critical COVID−19 patients,[41] and Junqueria et al. have reported that FcγR-mediated SARS-CoV−2 uptake by monocytic cells triggers inflammatory cell death and causes systemic inflammation.[42] Therefore, although serious adverse events due to FcγR-mediated inflammatory responses have not been reported in patients administered anti-SARS-CoV−2 therapeutic mAbs, FcγR-mediated immune cell activation properties seem to be an important characteristic for considering the safety of anti-SARS-CoV−2 therapeutic mAbs. Using the IgG4 subclass or engineered IgG1 showing reduced effector functions is a promising strategy for reducing the risk of undesirable FcγR-mediated immune cell activation, and indeed, some anti-SARS-CoV−2 mAbs used in clinical studies (etesevimab, cilgavimab, and tixagevimab) have an engineered Fc region reducing antibody effector functions. In this study, we focused
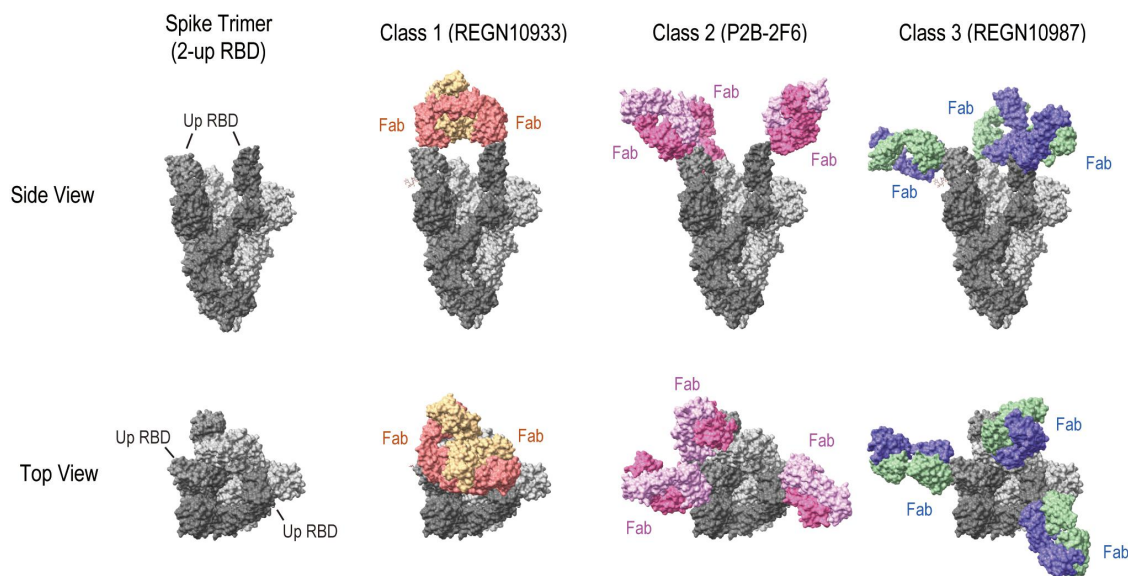

Figure 6. Structural models of anti-SARS-CoV −2 mAb Fab bound to a spike trimer. A spike trimer in two-up conformation (PDB ID: 6 × 2B) is shown as a gray surface ("up" RBDs, dark gray; "down" RBDs, light gray). Binding models of REGN10933 (class 1), P2B − 2F6 (class 2) and REGN10987 (class 3) were generated using UCSF ChimeraX by superimposing structures (REGN10933/REGN10987: 6×DG, P2B − 2F6: 7BWJ). Fab molecules are shown as colored surfaces.

on the differences in the binding epitopes (binding classes) of anti-SARS-CoV−2 mAbs, and tried to reduce the influence of the differences in antibody Fc regions. Thus, we used FcγRIIa-expressing reporter cells for measuring FcγR-activation by immune complexes because it is known that mAbs' binding affinities to FcγRIIa are less affected by the differences in Fc structures, including glycan compositions. On the other hand, FcγRIIIa-binding affinities are affected by afucosylated glycans at Fc region, and Fc glycan compositions of IgGs are varied depending on expression systems used for the preparation of recombinant IgG. Fc glycan compositions of human IgGs in plasma are known to be varied dependent on immunological conditions, and the involvement of FcγRIIIa activation in immunopathology of COVID−19 has been reported.[41,42] Therefore, when analyzing clinical samples, the differences in the FcγR-binding properties affected by the Fc structures and their impacts on FcγR-mediated immune cell activations should be considered.

There are some limitations of this study. We evaluated FcγR-activation properties using SARS-CoV−2 pseudo-typed lentivirus, not the authentic virus. It is unknown whether the characteristics of spike proteins (e.g., the membrane surface density or the conformation of trimeric spike proteins) in pseudo-typed virus accurately reflect those in the authentic virus. The characteristics of immune complexes (e.g., the size or FcγR-activation property) formed by mAbs bound to the pseudo-typed virus could differ from those bound to the authentic virus. Further experiments using both the pseudo-typed virus and the authentic virus are required for characterizing the size and FcγR-activation properties of immune complexes and revealing the differences among the binding classes of anti-SARS-CoV−2 mAbs. As reviewed by Corti et al.,[3] the roles of Fc-dependent effector functions of anti-SARS-CoV−2 mAbs in humans are not fully understood. Further studies are required to understand the impacts of FcγR-mediated immune cell activation, as well as other Fc-dependent effector functions, on the efficacy and safety of anti-SARS-CoV−2 mAbs.

In conclusion, we analyzed the biological activities of anti-SARS-CoV−2 mAbs using a panel consisting of 31 mAbs. Our approach was useful for revealing the characteristics of mAbs in each binding class in relation to the major SARS-CoV−2 variant mutations. In particular, our structural investigations of the differences in the FcγR-activation property of immune-complexes should be a key finding for considering the clinical impacts of anti-SARS-CoV−2 mAbs.

Materials and methods

Preparation of recombinant anti-SARS-CoV−2 mAbs

Amino acid sequences of anti-SARS-CoV−2 mAbs were obtained from public sources (PDB (www.rcsb.org/) or INN (www.who.int/teams/health-product-and-policy-standards /inn/inn-lists)). cDNAs corresponding to the variable regions of antibody heavy chains (VH) and light chains (VL) were synthesized (Genscript), then subcloned into pFUSE-CHIg-hG1, pFUSE2-CLIg-hK and pFUSE2-CLIg-hL2 vectors (Invivogen) for expressing the heavy chain, kappa light chain, and lambda light chain of human IgG1, respectively.

Recombinant mAbs were produced using the ExpiCHO Expression System (Thermo, #A29133) according to the manufacturer's protocol. Briefly, ExpiCHO cells were transiently transfected with antibody heavy-chain and light-chain expression vectors and cultured for 7–10 days. The culture supernatants were collected by centrifugation, and recombinant mAbs were purified using a HiTrap Protein A column (Cytiva, #29048576). Protein concentration was estimated by the absorbance at 280 nm measured by a NanoDrop spectrophotometer (Thermo). The purities of mAbs were > 95% estimated by size-exclusion chromatography (data not shown). Rituximab (Rituxan, Chugai Pharmaceutical) was obtained via a reagent supplier and used as a negative control.

SPR analysis

A Biacore 8K instrument (Cytiva) and Biotin CAPture Kit (Cytiva, #28920234) were used to evaluate the binding of anti-SARS-CoV−2 mAbs to SARS-CoV−2 spike proteins. All measurements were performed at 25°C, and HBS-EP+ (Cytiva, #BR100669) was used as a running buffer. Biotinylated SARS-CoV−2 spike S1 protein (Sino Biologicals, #40591-V27H-B) was captured on the Sensor Chip CAP, and then serially diluted anti-SARS-CoV−2 mAbs were sequentially injected into the flow cells. Association (k_{on}) and dissociation (k_{off}) rate constants were calculated by single-cycle analysis using the 1:1 binding model.

ECL multiplex assay

Binding and neutralization activities of mAbs against SARS-CoV−2 variant spike proteins were measured by ECL multiplex assay using a V-PLEX SARS-CoV−2 Panel 23 Kit (Meso Scale Discovery). In this assay plate, the wells were coated with SARS-CoV−2 spike proteins from the following lineages: WT (Wuhan), Alpha (B.1.1.7), Beta (B.1.351), Gamma (P.1), Delta (B.1.617.2; AY.4, B.1.617.2; AY.4.2 and B.1.617.2; AY.3; AY.5; AY.6; AY.7; AY.14) and Omicron (B.1.1.529; BA.1). Measurements were performed according to the manufacturer's instructions. To evaluate the binding activities, each well of a SARS-CoV−2 Plate 23 was blocked with 5% Blocker A in MSD phosphate buffer for 30 min. After washing with MSD Wash Buffer, serially diluted mAbs were added to each well and incubated for 1 h with shaking. After washing the plate, SULFO-TAG anti-human IgG Fc solution was added to each well and incubated for 1 h with shaking. The plates were washed and MSD GOLD Read Buffer B was added to each well, followed by the detection of ECL signals using MESO QuickPlex SQ120 (Meso Scale Discovery). For evaluating neutralization activities, sample-treated plates were incubated with SULFO-TAG human ACE2 protein detection solution for 1 h with shaking, and the ECL signals were measured as described above. The percentages of neutralization were calculated by normalizing ECL signals of each sample to that of the control sample. The binding ECL signals or the percentages of neutralization were plotted against the concentration of anti-SARS-CoV−2 mAbs, and AUCs of each dose – response curve were calculated using GraphPad Prism 6 software (GraphPad

Software). The curves above the baseline were used for calculating AUCs.

Preparation of SARS-CoV−2 spike pseudo-typed virus and neutralization assay

Pseudo-typed virus bearing the SARS-CoV−2 spike protein was produced based on the third-generation lentivirus system. Lenti-X 293T cells were obtained from Takara Bio and cultured in high-glucose DMEM (Thermo, #10569–044) supplemented with 10% fetal bovine serum (FBS) at 37°C in a humidified atmosphere containing 5% CO_2. pRSV-Rev (Addgene #12253) and pMDLg/pRRE (Addgene # 12251) were gifts from Didier Trono.[43] pcDNA3.1- spike_del19 (Addgene #155297) was a gift from Raffaele De Francesco. pLV-neo-CMV-EGFP was obtained from VectorBuilder. Lenti-X 293T cells were seeded in a 100-mm collagen-coated dish (7.5×10^6 cells/dish), cultured for 20 h, and transfected with 6.6 µg of pMDLg/pRRE, 3.3 µg of pRSV-Rev, 3.3 µg of pcDNA3.1- spike_del19 and 4.3 µg of pLV-neo-CMV-EGFP using Lipofectamine 3000 reagent (Thermo, #L3000008). After 6 h of culture, the medium was removed, and 10 mL of Opti-MEM Reduced Serum Medium (Thermo, #51985–034) supplemented with 5% FBS was added to the dish, and the cells were further incubated for 46 h. The culture supernatant was collected and filtered through a 0.45 µm filter, and then concentrated using Lenti-X Concentrator (Takara Bio, #631232). The viral titer (the amount of p24) was estimated using Lenti-X GoStix Plus (Takara Bio, #631280) following the manufacturer's instruction.

Neutralization assays against the pseudo-typed viruses were performed using Human ACE2 293T cells (Takara Bio) as the target cells. These cells were seeded into a collagen-coated 96-well plate (5×10^3 cells/well) and incubated for 24 h. After removing the medium, the cells were treated with the pseudo-typed virus (20 ng of p24/well) in the presence of serially diluted anti-SARS-CoV−2 mAbs for 6 h. After the medium was removed, fresh medium was added to wells, and the cells were further cultured for 96 h. Percentages of infection were estimated from EGFP-positive populations analyzed by a FACSCanto II Flow Cytometer (BD Biosciences), and the neutralization activities (%) were calculated by normalizing the data of each mAb-treated sample to that of an mAb-untreated sample.

Measurement of FcγRIIa activation by immune complexes

Jurkat-expressing human FcγRIIa cells with Nuclear Factor of Activated T cells (NFAT)-driven luciferase reporter (Jurkat/FcγRIIa/NFAT-Luc) were established previously,[39] and were used as a reporter cell line for measuring FcγRIIa activation. Immune complexes were prepared by incubating 10 µL of anti-SARS-CoV−2 mAbs (10 µg/mL) with 40 µL of SARS-CoV−2 pseudo-typed virus (375 ng of p24/mL) in Opti-MEM Reduced Serum Medium for 30 min at 37°C. Jurkat/FcγRIIa/NFAT-Luc cells were seeded into the wells of a 96-well round-bottom plate (1×10^5 cells/50 µL/well), then treated with 50 µL of the immune complexes and incubated for 5 h at 37°C. The

luciferase activities were measured using a ONE-Glo Luciferase Assay Reagent (Promega, #E6110) and an Ensight multimode plate reader (PerkinElmer).

Abbreviations

ACE2	angiotensin-converting enzyme 2
AUC	area under the curve
COVID−19	coronavirus disease 2019
ECL	electrochemiluminescence
FBS	fetal bovine serum
FcγR	Fcγ receptor
INN	International Nonproprietary Names
MAbs	monoclonal antibodies
NFAT	nuclear factor of activated T cells
NGS	next-generation sequencing
NTD	N-terminal domain
PDB	Protein Data Bank
RBD	receptor-binding domain
RBM	receptor-binding motif
SARS-CoV−2	severe acute respiratory syndrome coronavirus 2
SPR	surface plasmon resonance
VOCs	variants of concern

ORCID

Minoru Tada http://orcid.org/0000-0003-4739-1259

References

1. Pantaleo G, Correia B, Fenwick C, Joo VS, Perez L. Antibodies to combat viral infections: development strategies and progress. Nat Rev Drug Discov. 2022;21:676–96. doi:10.1038/s41573-022-00495-3. PMID: 35725925.
2. Ferrara F, D'Angelo S, Erasmus MF, Teixeira AA, Leal-Lopes C, Spector LP, Pohl T, Fanni A, Cocklin S, Bradbury ARM. Pandemic's silver lining. MAbs. 2022;14:2133666. doi:10.1080/19420862.2022.2133666. PMID: 36253351.
3. Corti D, Purcell LA, Snell G, Veesler D. Tackling COVID-19 with neutralizing monoclonal antibodies. Cell. 2021;184(12):3086–108. PMID: 34087172. doi:10.1016/j.cell.2021.05.005.

4. Focosi D, McConnell S, Casadevall A, Cappello E, Valdiserra G, Tuccori M. 2022. Monoclonal antibody therapies against SARS-CoV-2. The lancet infectious diseases. PMID: 35803289 22 (11):e311–e26. doi:10.1016/S1473-3099(22)00311-5

5. Ismail AM, Elfiky AA. 2020. SARS-CoV-2 spike behavior in situ: a Cryo-EM images for a better understanding of the COVID-19 pandemic. Signal transduction and targeted therapy. PMID: 33127886 5(1):252. doi:10.1038/s41392-020-00365-7

6. Ke Z, Oton J, Qu K, Cortese M, Zila V, McKeane L, Nakane T, Zivanov J, Neufeldt CJ, Cerikan B, et al. Structures and distributions of SARS-CoV-2 spike proteins on intact virions. Nature. 2020;588(7838):498–502. doi:10.1038/s41586-020-2665-2. PMID: 32805734.

7. Deshpande A, Harris BD, Martinez-Sobrido L, Kobie JJ, Walter MR. Epitope classification and RBD binding properties of neutralizing antibodies against SARS-CoV-2 variants of concern. Front Immunol. 2021;12:691715. doi:10.3389/fimmu.2021.691715. PMID: 34149735.

8. Finkelstein MT, Mermelstein AG, Parker Miller E, Seth PC, Stancofski ED, Fera D. Structural analysis of neutralizing epitopes of the SARS-CoV-2 spike to guide therapy and vaccine design strategies. Viruses. 2021;13(1):134. PMID: 33477902. doi:10.3390/v13010134.

9. Goddard TD, Huang CC, Meng EC, Pettersen EF, Couch GS, Morris JH, Ferrin TE. UCSF ChimeraX: meeting modern challenges in visualization and analysis. Protein Sci. 2018;27(1):14–25. PMID: 28710774. doi:10.1002/pro.3235.

10. Pettersen EF, Goddard TD, Huang CC, Meng EC, Couch GS, Croll TI, Morris JH, Ferrin TE. UCSF ChimeraX: structure visualization for researchers, educators, and developers. Protein Sci. 2021;30(1):70–82. PMID: 32881101. doi:10.1002/pro.3943.

11. Carabelli AM, Peacock TP, Thorne LG, Harvey WT, Hughes J, Peacock SJ, Barclay WS, Barclay, de Silva TI TI, Towers GJ, et al. SARS-CoV-2 variant biology: immune escape, transmission and fitness. Nat Rev Microbiol. 2023;1–16. PMID: 36653446. doi:10.1038/s41579-022-00841-7.

12. Scovino AM, Dahab EC, Vieira GF, Freire-de-Lima L, Freire-de-Lima CG, Morrot A. SARS-CoV-2's variants of concern: a brief characterization. Front Immunol. 2022;13:834098. doi:10.3389/fimmu.2022.834098. PMID: 35958548.

13. Chakraborty C, Sharma AR, Bhattacharya M, Lee SS. A detailed overview of immune escape, antibody escape, partial vaccine escape of SARS-CoV-2 and their emerging variants with escape mutations. Front Immunol. 2022;13:801522. doi:10.3389/fimmu.2022.801522. PMID: 35222380.

14. Cox M, Peacock TP, Harvey WT, Hughes J, Wright DW, Willett BJ, Thomson E, Gupta RK, Peacock SJ, Robertson DL, et al. SARS-CoV-2 variant evasion of monoclonal antibodies based on in vitro studies. Nat Rev Microbiol. 2023;21(2):112–24. doi:10.1038/s41579-022-00809-7. PMID: 36307535.

15. Greaney AJ, Loes AN, Crawford KHD, Starr TN, Malone KD, Chu HY, Bloom JD. Comprehensive mapping of mutations in the SARS-CoV-2 receptor-binding domain that affect recognition by polyclonal human plasma antibodies. Cell Host & Microbe. 2021;29(3):463–476.e6. PMID: 33592168. doi:10.1016/j.chom.2021.02.003.

16. Yang WT, Huang WH, Liao TL, Hsiao TH, Chuang HN, Liu PY. SARS-CoV-2 E484K mutation narrative review: epidemiology, immune escape, clinical implications, and future considerations. Infect Drug Resist. 2022;15:373–85. doi:10.2147/IDR.S344099. PMID: 35140483.

17. Cao Y, Wang J, Jian F, Xiao T, Song W, Yisimayi A, Huang W, Li Q, Wang P, An R, et al. Omicron escapes the majority of existing SARS-CoV-2 neutralizing antibodies. Nature. 2022;602 (7898):657–63. doi:10.1038/s41586-021-04385-3. PMID: 35016194.

18. Shah M, Woo HG. Omicron: a heavily mutated SARS-CoV-2 variant exhibits stronger binding to ACE2 and potently escapes approved COVID-19 therapeutic antibodies. Front Immunol. 2021;12:830527. doi:10.3389/fimmu.2021.830527. PMID: 35140714.

19. Deng X, Garcia-Knight MA, Khalid MM, Servellita V, Wang C, Morris MK, Sotomayor-Gonzalez A, Glasner DR, Reyes KR, Gliwa AS, et al. Transmission, infectivity, and neutralization of a spike L452R SARS-CoV-2 variant. Cell. 2021;184(13):3426–37. e8. doi:10.1016/j.cell.2021.04.025. PMID: 33991487.

20. Li Q, Wu J, Nie J, Zhang L, Hao H, Liu S, Zhao C, Zhang Q, Liu H, Nie L, et al. The impact of mutations in SARS-CoV-2 spike on viral infectivity and antigenicity. Cell. 2020;182(5):1284–94.e9. doi:10.1016/j.cell.2020.07.012. PMID: 32730807.

21. Hansen J, Baum A, Pascal KE, Russo V, Giordano S, Wloga E, Fulton BO, Yan Y, Koon K, Patel K, et al. Studies in humanized mice and convalescent humans yield a SARS-CoV-2 antibody cocktail. Science. 2020;369(6506):1010–14. doi:10.1126/science.abd0827. PMID: 32540901.

22. Yuan M, Wu NC, Zhu X, Lee CD, So RTY, Lv H, Mok CKP, Wilson IA. A highly conserved cryptic epitope in the receptor binding domains of SARS-CoV-2 and SARS-CoV. Science. 2020;368(6491):630–33. PMID: 32245784. doi:10.1126/science.abb7269.

23. Ju B, Zhang Q, Ge J, Wang R, Sun J, Ge X, Yu J, Shan S, Zhou B, Song S, et al. Human neutralizing antibodies elicited by SARS-CoV-2 infection. Nature. 2020;584(7819):115–19. doi:10.1038/s41586-020-2380-z. PMID: 32454513.

24. Pinto D, Park YJ, Beltramello M, Walls AC, Tortorici MA, Bianchi S, Jaconi S, Culap K, Zatta F, De Marco A, et al. Cross-neutralization of SARS-CoV-2 by a human monoclonal SARS-CoV antibody. Nature. 2020;583(7815):290–95. doi:10.1038/s41586-020-2349-y. PMID: 32422645.

25. Cao Y, Su B, Guo X, Sun W, Deng Y, Bao L, Zhu Q, Zhang X, Zheng Y, Geng C, et al. Potent neutralizing antibodies against SARS-CoV-2 identified by high-throughput single-cell sequencing of convalescent patients' B cells. Cell. 2020;182(1):73–84.e16. doi:10.1016/j.cell.2020.05.025. PMID: 32425270.

26. Wu Y, Wang F, Shen C, Peng W, Li D, Zhao C, Li Z, Li S, Bi Y, Yang Y, et al. A noncompeting pair of human neutralizing antibodies block COVID-19 virus binding to its receptor ACE2. Science. 2020;368(6496):1274–78. doi:10.1126/science.abc2241. PMID: 32404477.

27. Shi R, Shan C, Duan X, Chen Z, Liu P, Song J, Song T, Bi X, Han C, Wu L, et al. A human neutralizing antibody targets the receptor-binding site of SARS-CoV-2. Nature. 2020;584 (7819):120–24. doi:10.1038/s41586-020-2381-y. PMID: 32454512.

28. Rujas E, Kucharska I, Tan YZ, Benlekbir S, Cui H, Zhao T, Wasney GA, Budylowski P, Guvenc F, Newton JC, et al. Multivalency transforms SARS-CoV-2 antibodies into ultrapotent neutralizers. Nat Commun. 2021;12(1):3661. doi:10.1038/s41467-021-23825-2. PMID: 34135340.

29. Barnes CO, Jette CA, Abernathy ME, Dam KA, Esswein SR, Gristick HB, Malyutin AG, Sharaf NG, Huey-Tubman KE, Lee YE, et al. SARS-CoV-2 neutralizing antibody structures inform therapeutic strategies. Nature. 2020;588(7839):682–87. doi:10.1038/s41586-020-2852-1. PMID: 33045718.

30. Kreye J, Reincke SM, Kornau HC, Sanchez-Sendin E, Corman VM, Liu H, Yuan M, Wu NC, Zhu X, Lee CD, et al. A therapeutic non-self-reactive SARS-CoV-2 antibody protects from lung pathology in a COVID-19 hamster model. Cell. 2020;183 (4):1058–69.e19. doi:10.1016/j.cell.2020.09.049. PMID: 33058755.

31. Piccoli L, Park YJ, Tortorici MA, Czudnochowski N, Walls AC, Beltramello M, Silacci-Fregni C, Pinto D, Rosen LE, Bowen JE, et al. Mapping neutralizing and immunodominant sites on the SARS-CoV-2 spike receptor-binding domain by structure-guided high-resolution serology. Cell. 2020;183(4):1024–42.e21. doi:10.1016/j.cell.2020.09.037. PMID: 32991844.

32. Tortorici MA, Beltramello M, Lempp FA, Pinto D, Dang HV, Rosen LE, McCallum M, Bowen J, Minola A, Jaconi S, et al. Ultrapotent human antibodies protect against SARS-CoV-2 challenge via multiple mechanisms. Science. 2020;370(6519):950–57. doi:10.1126/science.abe3354. PMID: 32972994.

33. Chi X, Yan R, Zhang J, Zhang G, Zhang Y, Hao M, Zhang Z, Fan P, Dong Y, Yang Y, et al. A neutralizing human antibody binds to the

N-terminal domain of the Spike protein of SARS-CoV-2. Science. 2020;369(6504):650–55. doi:10.1126/science.abc6952. PMID: 32571838.

34. Lv Z, Deng YQ, Ye Q, Cao L, Sun CY, Fan C, Huang W, Sun S, Sun Y, Zhu L, et al. Structural basis for neutralization of SARS-CoV-2 and SARS-CoV by a potent therapeutic antibody. Science. 2020;369(6510):1505–09. doi:10.1126/science.abc5881. PMID: 32703908.

35. Bournazos S, Ravetch JV. Fcgamma receptor pathways during active and passive immunization. Immunol Rev. 2015;268:88–103. doi:10.1111/imr.12343. PMID: 26497515.

36. Nimmerjahn F, Ravetch JV. Fcγ receptors as regulators of immune responses. Nat Rev Immunol. 2008;8(1):34–47. PMID: 18064051. doi:10.1038/nri2206.

37. Tada M, Aoyama M, Ishii-Watabe A. Fcγ receptor activation by human monoclonal antibody aggregates. J Pharm Sci. 2020;109 (1):576–83. PMID: 31676270. doi:10.1016/j.xphs.2019.10.046.

38. Tada M, Suzuki T, Ishii-Watabe A. Development and characterization of an anti-rituximab monoclonal antibody panel. MAbs. 2018;10(3):370–79. PMID: 29309213. doi:10.1080/19420862.2018. 1424610.

39. Tada M, Ishii-Watabe A, Suzuki T, Kawasaki N, Zhou P. Development of a cell-based assay measuring the activation of FcγRIIa for the characterization of therapeutic monoclonal antibodies. PLos One. 2014;9(4):e95787. PMID: 24752341. doi:10. 1371/journal.pone.0095787.

40. Huo J, Zhao Y, Ren J, Zhou D, Duyvesteyn HME, Ginn HM, Carrique L, Malinauskas T, Ruza RR, Shah PNM, et al. Neutralization of SARS-CoV-2 by destruction of the prefusion spike. Cell Host & Microbe. 2020;28:497. doi:10.1016/j.chom. 2020.07.002. PMID: 32910920.

41. Ankerhold J, Giese S, Kolb P, Maul-Pavicic A, Voll RE, Goppert N, Ciminski K, Kreutz C, Lother A, Salzer U, et al. Circulating multimeric immune complexes contribute to immunopathology in COVID-19. Nat Commun. 2022;13:5654. doi:10.1038/s41467-022-32867-z. PMID: 36163132.

42. Junqueira C, Crespo A, Ranjbar S, de Lacerda LB, Lewandrowski M, Ingber J, Parry B, Ravid S, Clark S, Schrimpf MR, et al. FcγR-mediated SARS-CoV-2 infection of monocytes activates inflammation. Nature. 2022;606 (7914):576–84. doi:10.1038/s41586-022-04702-4. PMID: 35385861.

43. Dull T, Zufferey R, Kelly M, Mandel RJ, Nguyen M, Trono D, Naldini L. A third-generation lentivirus vector with a conditional packaging system. J Virol. 1998;72(11):8463–71. PMID: 9765382. doi:10.1128/JVI.72.11.8463-8471.1998.